NON-REACTIVE FLOWFIELD CHARACTERIZATION OF A NATURAL GAS BURNER FOR TURBULENT COMBUSTION STUDIES

Miguel Angel Alvarez Aquino, malvarez@mec.puc-rio.br
Luís Fernando Figueira da Silva, luisfer@mec.puc-rio.br
Luis Fernando Alzuguir Azevedo, lfaa@mec.puc-rio.br
Departamento de Engenharia Mecânica
Pontifícia Universidade Católica do Rio de Janeiro
Rua Marquês de São Vicente, 225
22453-900 Rio de Janeiro, RJ BRASIL

Abstract. *Turbulent non premixed combustion is found in several industrial applications, such as furnaces, boilers, gas turbines, etc. This work presents an experimental study of the characteristics of the structure of the turbulent non-reactive flowfield in a newly design Bluff Body burner. This natural gas/air burner has a simple cylindrical geometry and was designed with the purpose of allowing for the use of laser based diagnostic techniques. This type of burner has an extended range of safe operating conditions without necessity of a pilot flame. Furthermore, it has the advantage of stably anchoring of flames in high velocity flowfields. In this paper, we characterize, by means of non intrusive measurement techniques, i.e., Particle Image Velocimetry (PIV) and Laser Doppler Velocimetry (LDV) the radial and axial components of the velocity fields. The results obtained with these detailed measurement techniques are compared against computational fluid dynamics results.*

Keywords*: combustion, experimental study*

1. INTRODUCTION

This works presents a comparison between measured and computed velocity distributions of the chemically inert flowfield on a Bluff-Body type burner. It is the first part of an on-going effort to establish an indigenous database for the development and validation of turbulent combustion models. This type of burner, in which the combustion of non-premixed streams of natural gas and air is stabilized, is representative of burners which may be found in furnaces, boilers and gas turbines, for instance. Performance improvements, pollutants emissions reductions and fuel conversions of existing burners require the detailed understanding of turbulence/chemistry interactions. In the case of bluff-body burners flame anchoring is accomplished by a region of hot combustion products which reside at the vicinity of the bluff body surface, thus avoiding the use of pilot flames or swirl to ensure a large safe operational range. The simplicity of the geometrical configuration involved allows for ample optical access, which may be used for detailed flow characterization.

Indeed, starting with Roquemore et al. (1983), Schefer et al. (1987, 1989) and Masri et al. (1992, 1994), several authors have used this type of burner as an investigation tool devoted to the knowledge increase of turbulence/combustion interactions. To this end, different non-intrusive laser based techniques have been used, such as Laser Doppler Velocimetry, Laser Induced Fluorescence of various combustion radicals, Coherent Anti-Stokes Raman Spectroscopy, to quote a few. Masri et al. (1996) have summarized the early work on the subject. Recent information on the subject has been compiled at a series of Turbulent Non-premixed Flames workshops (TNF, 2007).

In this work are briefly presented the bluff body burner developed, the Particle Image Velocimetry (PIV) and Laser Doppler Velocimetry (LDV) measurement techniques and the computational methodology. Then, the overall flow structure is discussed. Finally, the results obtained with these methodologies are compared in terms of averaged and fluctuating velocity components.

2. THE BLUFF BODY BURNER

The bluff body burner built during the present study is shown in Fig. 1. An outer stream of air exits a 200 mm diameter duct, thus surrounding a 36 mm diameter bluff body which has a 2 mm diameter orifice at its center. Either fuel or air may exit through this central orifice. Natural gas was used successfully to investigate the possible combustion regimes (Alvarez Aquino, 2006), which range from laminar diffusion flames to turbulent, lifted, partially premixed combustion. This work presents the results of the initial characterization of such a burner, which was performed by considering the flow of air through the central orifice. The central jet Reynolds number used was Re_j=3870, which corresponds to an averaged flow velocity of U_j=27.5 m/s. The outer air velocity was 1.5 m/s, as measured by the LDV and PIV systems. During the tests, the average ambient temperature was around 20 ºC and the averaged humidity 64 %.

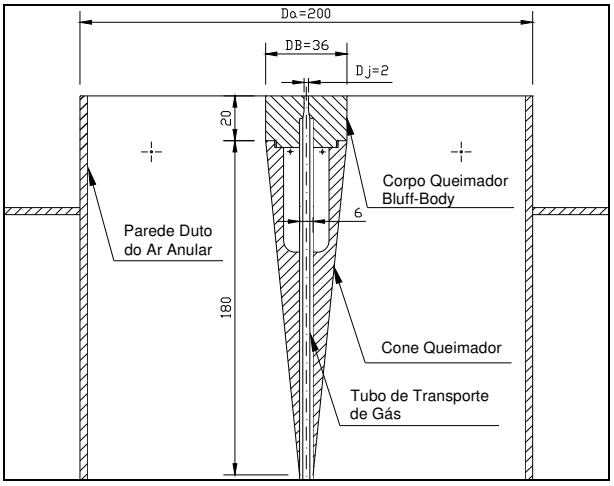

Figure 1. Experimental facility schematics (dimensions in mm).

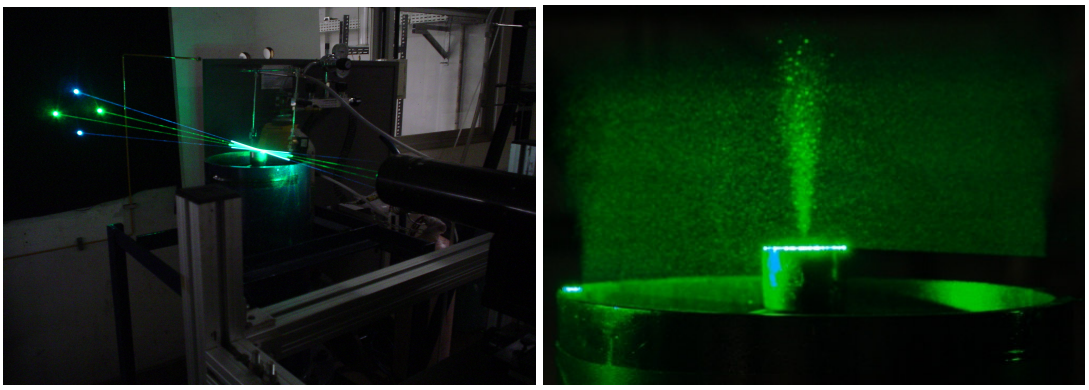

Figure 2. Experimental facility while using the (b) LDV technique and (b) PIV technique.

3. MEASUREMENT TECHNIQUES

In this work the flowfield velocity is characterized by two laser-based techniques, the laser Doppler velocimetry (LDV) and the particle imaging velocimetry, which measure the velocity of particles which are carried by the air flow. Here a Laskin nozzle atomizer was used to disperse oil droplets in both air streams, with diameter of the order of 1 μm (Abrantes, 2005). The velocity of these particles is identical to the local, instantaneous, flow velocity for the experimental conditions considered here. For the sake of brevity, only the main features of these measurement techniques are outlined below.

3.1. Laser Doppler Velocimetry

A two-color LDV system, manufactured by TSI, Inc., was used in this work to measure the longitudinal and radial components of the velocity vector. This system, part of which may be seen in Fig. 2, uses the 514.5 nm and 488 nm wavelengths of a 5 W argon laser to produce two pairs of laser beams which interfere within a measurement volume with dimensions of 100 x 250 μm^2. A Bragg cell is used to frequency-shift one of the beams of each wavelength in order to allow for directional velocity measurements. After collection by the receiver, the back-scattered light is digitally processed (IFA 755-2, TSI, Inc.) and the resulting signal is post-processed by the software FIND (FFW1.4, TSI, Inc.). The measurement volume is displaced by means of a three-component coordinate table equipped with a digital meter with a resolution of 0.01 mm.. An uncertainty analysis was performed, accounting for the contributions of the LDV system, displacement of the measurement volume and jet flow Reynolds number on the measurement error. Considering that each measurement consisted of more than 10,000 samples, the total uncertainty associated with the determination of either component of averaged or RMS velocity was smaller than 1.7 %. However, the uncertainty associated with the Reynolds number, which is directly connected to the flow rate measurement uncertainty, and with the displacement table was 12 %.

3.2. Particle Image Velocimetry

The particle imaging velocimetry system used to measure velocity in a planar field uses a pair of pulsed (15 Hz) Nd-YAG lasers (532 nm harmonics) to illuminate the flowfield with a 60 mm × 0,20 mm laser sheet which passes through the center of the jet, as can be verified in Fig. 2. The scattered light from the particles is collected with a 4 MPixel, Power View Plus (TSI, Inc.) camera equipped with a 105-mm Nikor lens. The images were processed with the Insight 3G software (TSI, Inc.). With this camera placed 400 mm away from the jet centerline, the field of view was of 45.18 mm^2, leading to a 22.08 μm/pixel resolution along each direction. The influence of the choice of the time interval between pulses was investigated, which led to the choice of 5 μs, which better characterizes the jet flow, and 80 μs, which is more suited to measure the slower outer air flow and the recirculation region. All the results shown here correspond to the post-processing of 800 pairs of images. A detailed assessment of uncertainty with this measurement technique for the present experimental setup is still to be performed.

4. COMPUTATIONAL METHODOLOGY

The computational fluid dynamics (CFD) modeling of the inert flowfield of interest was performed by solving the Reynolds averaged transport equations of mass and momentum and using an axi-symmetric hypothesis. Closure of the Reynolds stress tensor was performed using the SST model (Menter, 1994). This model was chosen upon comparison of available two-equation eddy viscosity models with the experimental results of Schefer et al. (1987). The governing equations were discretized by a second-order finite volume technique and solved via a classical pressure-correction method. To this purpose, the ANSYS/CFX-10 computer code was used. The computational mesh contained 186 and 290 nodes along the longitudinal and radial directions, with a minimum spacing of 0.244 and 0.84 mm, respectively. The total extension of the computation domain is 450 ×115 mm^2, whereas a refined mesh region spans over 50 × 20 mm^2. Concerning the boundary conditions, uniform flow velocity with a turbulence intensity of 1 % was prescribed along the jet and air boundaries. The bluff body surface is considered to be a no-slip wall, and symmetry is imposed along the jet centerline. The remaining boundaries of the computational domain are treated as open boundaries, which flow direction and velocity value result from the entrainment of external fluid into the domain.

5. RESULTS AND DISCUSSION

5.1. Flow structure

Figure 3, which shows the distribution of averaged velocity modulus, averaged radial velocity and of the longitudinal and radial components of the turbulent intensity at the symmetry plane of the experiment, illustrates the overall structure of the flowfield. These results have been obtained by the PIV technique with a time lapse between laser pulses of 5 μs. For the chosen values of jet and co-flow velocities, the flow evolution is found to be dominated by the jet. Nevertheless, the averaged streamlines, which are superimposed to this figure, clearly show the presence of a toroidal vortex which is nearly symmetric around the $r=0$ axis. Note that the width of the recirculation region along the radial direction is controlled by the bluff body diameter, whereas the length of this recirculation region is approximately one bluff body radius, consistently with findings from other authors (Masri et al., 1996). The departure from the symmetry, which can be better assessed by examining the averaged radial velocity evolution, may be connected to a poor alignment of the bluff body face with the horizontal plane. On the basis of this result, a new alignment system was designed and is currently being installed. The turbulent intensities further indicate that the flow is of jet nature. Indeed, close to the bluff body face, the maximum values of these components arise at the vicinity of the jet boundary, where the velocity gradient is a maximum. As the jet develops further downstream and expands, these maximum values shift to the vicinity of the centerline and subsequently decrease, as the jet decays.

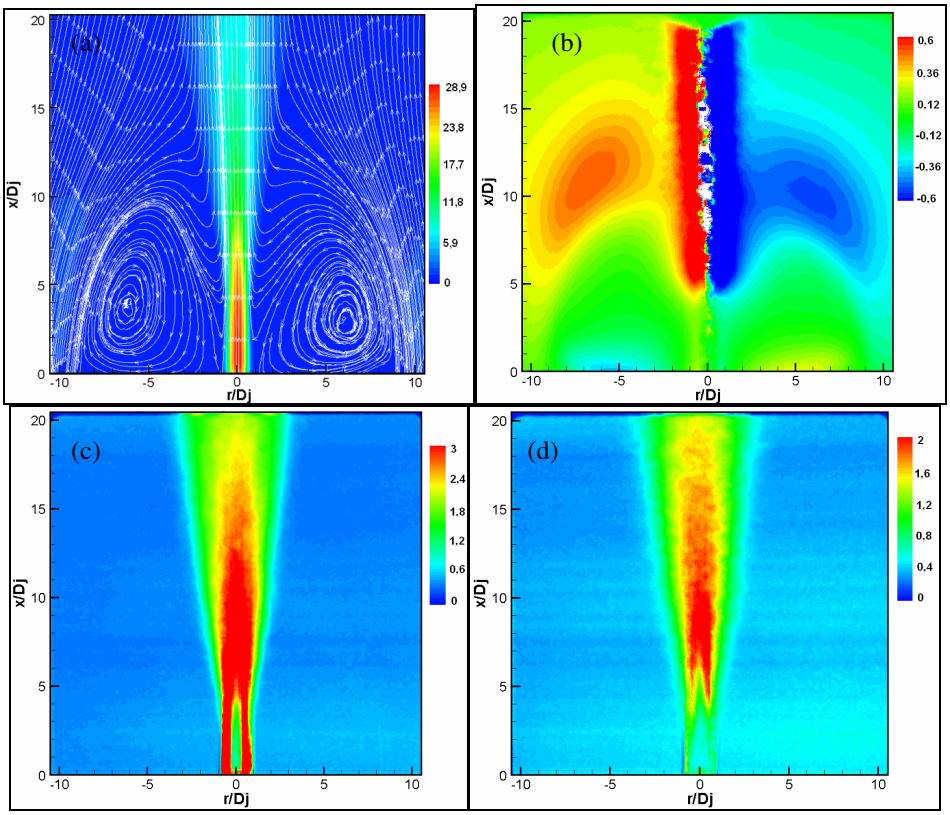

Figure 3. Contours of (a) averaged velocity modulus (m/s), with streamlines, (b) averaged radial velocity (m/s), (c) longitudinal velocity component turbulent intensity (m/s), (d) radial velocity component turbulent intensity (m/s). Results obtained using the PIV technique with a time lapse between laser pulses of 5 μs.

5.2. Flow properties evolutions along the centerline

The longitudinal evolution along the axis *r=0* of the averaged longitudinal velocity and of the turbulent intensity along the longitudinal and radial directions is shown in Fig. 4. This figure compares the experimental results obtained with both the LDV and the PIV techniques and the computational results obtained with the SST turbulence model. Concerning the longitudinal velocity component, this figure shows that an excellent agreement is observed between the measured values, whereas the computation yields a shorter length of the initial region of the jet. The subsequent computed decay ratio is in good agreement with the experimental values, however. This figure also shows that, during the initial jet development, important discrepancies exist on the turbulent intensity on the longitudinal and radial directions. Indeed, the intensity values obtained with the PIV technique, 4 and 2 %, respectively on the longitudinal and radial components, are higher than those corresponding to the LDV measurement, 2 and 1 %, and also than those specified at the computation with the SST isotropic turbulence model, 1%. The origin of such discrepancies among experimental values is under current scrutiny. Note, however, that the subsequent evolution of the measured intensities is nearly the same, until the region where intensity maxima are found. The measured longitudinal intensities decrease further downstream, whereas the radial intensity decreases in the case of the LDV measurement only. The abnormal behavior of the radial intensity obtained by the PIV technique could be explained by the peak-locking effect, where the particle displacement between frames is smaller than the pixel size of the camera, thus leading to an incorrect evaluation of the correlation between image pairs. Although the computed values of the intensity are in good qualitative agreement, a comparison between computed and measured results highlight the inadequacy of the isotropic hypothesis on the basis of eddy-viscosity models, such as the SST, for the simulation of the bluff body configuration.

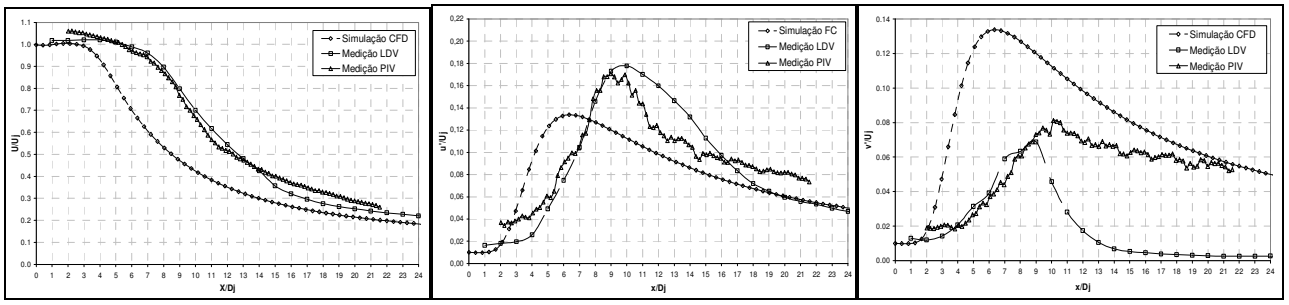

Figure 4. Comparisons between measured and computed evolutions along the longitudinal direction of the (a) longitudinal component of the averaged velocity, (b) RMS of the longitudinal component and (c) RMS of the radial component.

5.3. Radial evolution of the flow properties

The radial evolution of the averaged longitudinal velocity component at different longitudinal positions (x/D_j=1, 5, 10, 15 and 20) is shown in Fig. 5, where the results obtained by PIV and LDV techniques are compared to the computed ones. At the first longitudinal measurement position, x/D_j=1, the lateral extent of the jet, r/D_j=1.125, as computed and measured with the PIV technique are in excellent agreement. However, the LDV results show a jet which width is half that observed with the PIV technique, r/D_j=0.5, which is a clear indication that the LDV result at this position is an outlier. At this first position the presence of negative velocity values can be observed, which is characteristic of the recirculation zone. At the longitudinal position x/D_j=5, the PIV and LDV results exhibit a good agreement. In this position, minimum jet spread is yielded by the LDV technique, r/D_j=0.7, followed by the PIV, r/D_j=1.15, and by the CFD results. The larger computed spread of the jet is consistent with the faster decay of maximum averaged longitudinal velocity component seen in Fig. 4. Further downstream, LDV and PIV results show a better agreement. The maximum radial extent of the recirculation region at the longitudinal positions x/D_j=1 and 5, where it is mostly controlled by the bluff body dimension, is nearly identical for the PIV, LDV and CFD results.

Figure 6 compares the computed and measured radial distributions of the longitudinal turbulent intensity, u'/U_j, at different longitudinal positions, x/D_j=1, 5, 10, 15 and 20. At the first longitudinal position, the computed maximum value of turbulent intensity and the measurements performed with the PIV technique exhibit an excellent agreement. This highlights the ability of the SST turbulence model in predicting turbulent fluctuations in high shear regions, such as the mixing layer which exists between the jet and the recirculation region. The LDV measurement exhibits the smallest peak turbulent intensity value and mixing layer width, consistent with the under prediction of the jet averaged velocity. At the second longitudinal position, x/D_j= 5, large discrepancies can be observed both on the maximum turbulent intensity value and the total width of the shear region. Indeed, the maximum intensity measured with the LDV, computed with CFD and measured with the PIV, 0.08, 0.14, and 0.24, range from 1:3. The picture is rather different at x/D_j= 10: the results obtained with PIV and LDV exhibit a good agreement for r/D_j>1, and larger discrepancies for smaller radius. Further downstream, an abnormal behavior can be observed on the evolution of the turbulent intensity measured with LDV. This behavior may be explained by modifications on the frequency shift of one of the laser beams, which is used to determine the velocity. However, these results deserve further analysis. The experimental results obtained with the PIV technique and the computed evolutions of the turbulent intensity are shown to behave similarly at longitudinal positions x/D_j= 15 and 20, even though the actual values are different, as one could expect from the averaged longitudinal velocity component evolution.

6. ACKNOWLEDGEMENTS

This work was performed while the first author was a Master student with a CNPq scholarship, and the second author was on leave from *Laboratoire de Combustion et de Détonique* (*Centre National de la Recherche Scientifique*, France), with scholarships from CNPq (Profix) and ANP (visiting researcher). This work was supported by a CNPq/CT-Energ grant (process 401.310/2003-5).

7. REFERENCES

Abrantes, J. K., 2005, Estudo do Escoamento e Transferência de Calor em Jato Espiralado Incidente, Master Dissertation, Pontifícia Universidade Católica do Rio de Janeiro.

Masri, A. R., Dibble, R. W. and Barlow, R. S., 1992, "Raman-Rayleigh Measurements in Bluff-Body Stabilized Flames of Hidrocarbon Fuels", 24th Symposium International on Combustion, Pittsburgh, The Combustion Institute, pp. 317-324.

Masri, A. R., Dally, B. B., Barlow, R. S. and Carter, C. D., 1994, "The Structure of the Recirculation Zone of a Bluff-Body Combustor", 25th Symposium International on Combustion, Pittsburgh, The Combustion Institute, pp. 1301-1308.

Masri, A. R., Dibble, R.W. and Barlow, R.S., 1996, "The Structure of Turbulent Nonpremixed Flames revealed by Raman-Rayleigh-LIF Measurements", Progress in Energy and Combustion Science, vol. 22, pp. 307-362.

Menter, F. R., 1994, "Two-Equation Eddy-Viscosity Turbulence Models for Engineering Applications", AIAA Journal, Vol. 32, No. 8, pp. 1598-1605.

Roquemore, W. M., Bradley, R. P., Stutrud, J. S., Reeves, C. M. and Britton, R. L., 1983, "Influence of the Vortex Shedding Process on a Bluff-Body Difusion Flame", AIAA 21st Aerospace Sciences Meeting, AIAA Paper 83-0335.

Schefer, R. W., Namazian, M. and Kelly J., 1987, "Velocity Measurements in a Turbulent Nonpremixed Bluff-Body Stabilized Flame", Combustion Science and Technology, Vol. 56, No. 4-6, pp. 101-138.

Schefer, R. W., Namazian, M. and Kelly J., 1989, "Comparison of Turbulent-Jet and Bluff-Body Stabilized Flames", Combustion Science and Technology, Vol. 67, Nos. 4-6, pp. 123-146.

TNF, 2007, International Workshop on Measurement and Computation of Turbulent Non-Premixed Flames, http://www.ca.sandia.gov/TNF/abstract.html.

5. RESPONSIBILITY NOTICE

The authors are the only responsible for the printed material included in this paper.

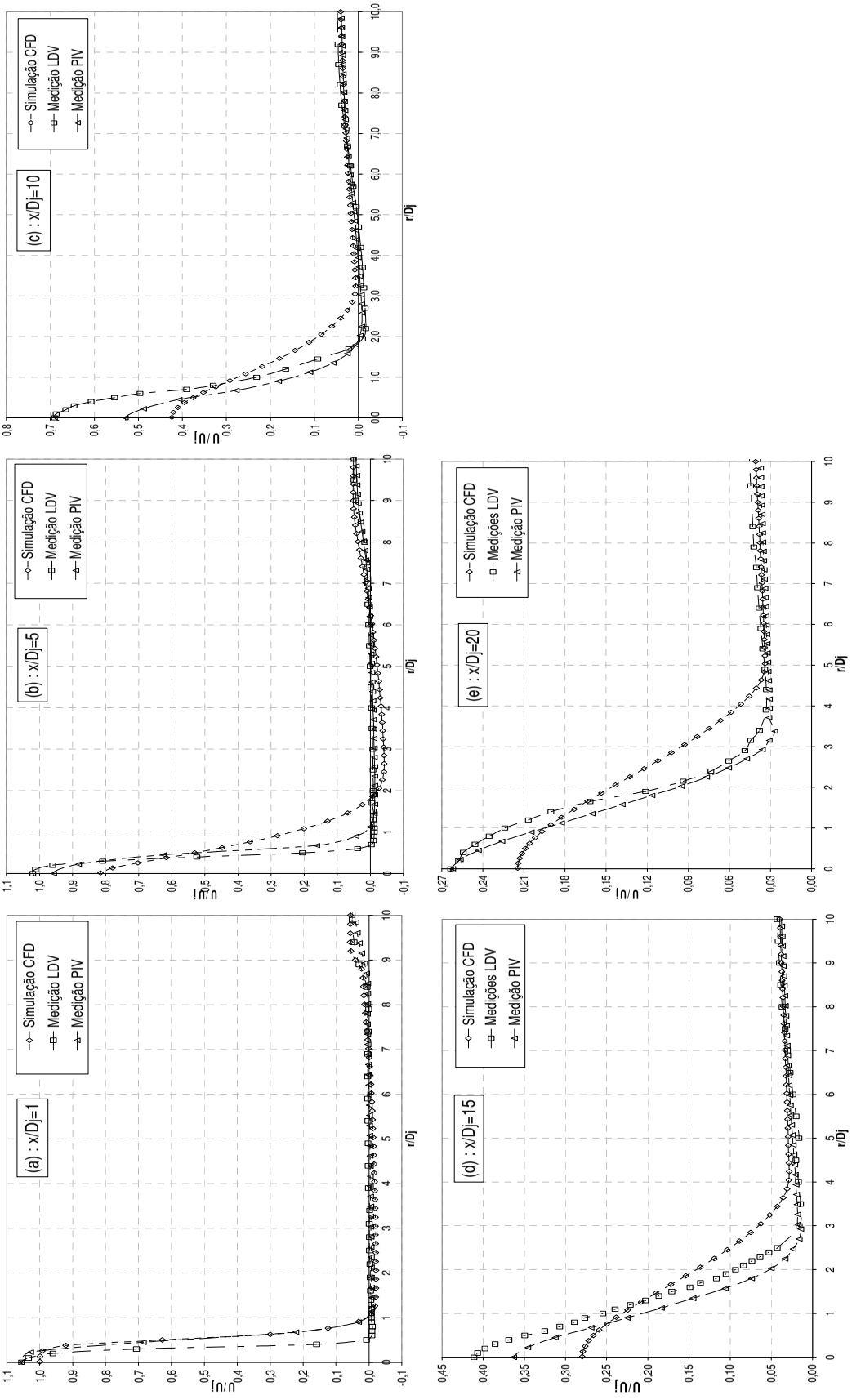

Figure 5. Comparisons between measured and computed radial distributions of the averaged longitudinal velocity component for different longitudinal positions.

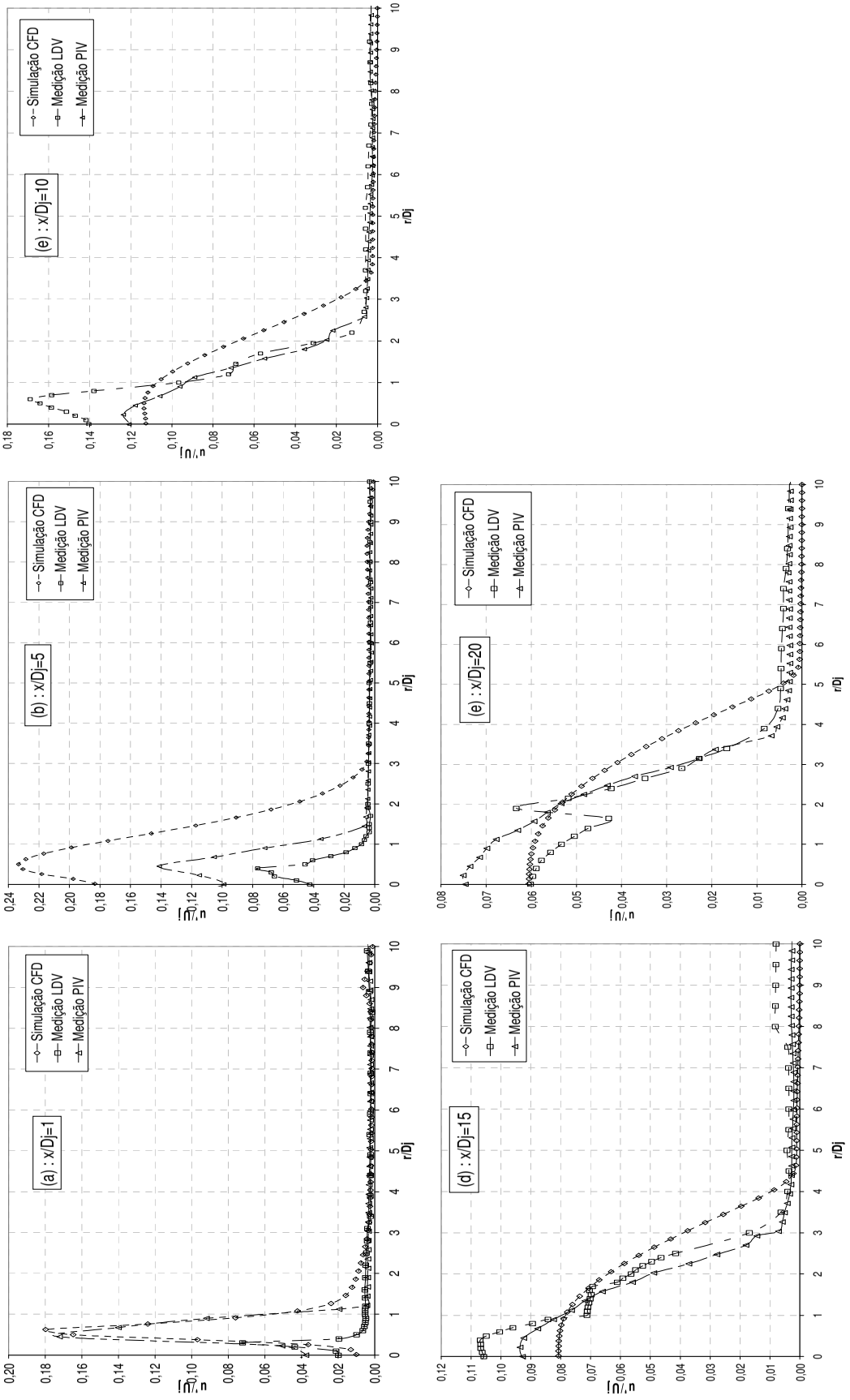

Figure 6. Comparisons between measured and computed radial distributions of the longitudinal velocity component turbulent intensity for different longitudinal positions.